

Research Project for the  
South Australian Mining and Quarrying Occupational Health and Safety Committee

# **FINAL REPORT**

**MAQ0520**

## **Understanding the Role of Organic Resin and Metal Ions in Artificial Stone Silicosis**

### **Principal Investigator**

Prof. Dino Pisaniello

### **Co-Investigators**

A/Prof. Sharyn Gaskin  
Dr Leigh Thredgold  
Dr Richie Gun  
Prof. Dusan Losic

**June 2021**

# The South Australian Mining and Quarrying Occupational Health and Safety Committee

## Disclaimer

**IMPORTANT:** The information in this guide is of a general nature, and should not be relied upon as individual professional advice. If necessary, legal advice should be obtained from a legal practitioner with expertise in the field of Work Health and Safety law (SA).

Although every effort has been made to ensure that the information in this guide is complete, current and accurate, the Mining and Quarrying Occupational Health and Safety Committee, any agent, author, contributor or the South Australian Government, does not guarantee that it is so, and the Committee accepts no responsibility for any loss, damage or personal injury that may result from the use of any material which is not complete, current and accurate.

Users should always verify historical material by making and relying upon their own separate inquiries prior to making any important decisions or taking any action on the basis of this information.

## Creative Commons



This work is licenced under  
***Creative Commons Attribution – Non Commercial 4.0 International  
Licence. The licence is available to view at  
<http://creativecommons.org/licenses/by-nc/4.0/>***

This creative commons licence allows you to copy, communicate and or adapt our work for non-commercial purposes only, as long as you attribute the work to Mining and Quarrying Occupational Health and Safety Committee and abide by all the other licence terms therein.

**ISBN 978-1-925361-92-6**

## Contact information

Mining and Quarrying Occupational Health and Safety Committee (MAQOHSC)  
Level 2, Torrens Building 220 Victoria Square  
Adelaide SA 5000  
Phone: (08) 8204 9842  
Email: [maqohsc@sa.gov.au](mailto:maqohsc@sa.gov.au)  
Website: [www.maqohsc.sa.gov.au](http://www.maqohsc.sa.gov.au)

## Table of Contents

|   |           |
|---|-----------|
| <b>1. Executive Summary</b>   | <b>4</b>  |
| <b>2. General Introduction</b>  | <b>8</b>  |
| <b>3. Initial Characterisation and Processing of Artificial Stone Samples</b>       | <b>10</b> |
| <b>4. Solubility Studies</b>  | <b>12</b> |
| <b>4.1 Preparation of Artificial Lysosomal Fluid</b>                                | <b>12</b> |
| <b>4.2 Organic Resin</b>  | <b>13</b> |
| 4.2.1 Introduction  |           |
| 4.2.2 Methods   |           |
| 4.2.3 Results   |           |
| 4.2.4 Interpretation  |           |
| <b>4.3 Metal Ions</b>   | <b>15</b> |
| 4.3.1 Introduction  |           |
| 4.3.2 Methods   |           |
| 4.3.3 Results   |           |
| 4.3.4 Interpretation  |           |
| <b>5. General Discussion</b>  | <b>17</b> |
| <b>6. Implications and Recommendations</b>  | <b>18</b> |
| <b>7. Acknowledgements</b>  | <b>20</b> |
| <b>8. References</b>  | <b>20</b> |
| <b>9. Appendices</b>  | <b>24</b> |
| <b>Appendix 1: Physicochemical characterisation of comminuted artificial stones</b> | <b>24</b> |
| <b>Appendix 1.1: Wet sizing of selected comminuted artificial stones</b>            | <b>25</b> |
| <b>Appendix 1.2: Mineralogical analyses of comminuted artificial stones</b>         | <b>29</b> |
| <b>Appendix 1.3: Elemental analyses of comminuted artificial stones</b>             | <b>31</b> |
| <b>Appendix 2: Organic analyses of selected comminuted artificial stones</b>        | <b>33</b> |
| <b>Appendix 3: Time trends of metal ion release in ALF</b>                          | <b>35</b> |

# 1. Executive Summary

## Introduction:

Artificial stone (AS), also known as engineered or composite stone, is typically a mixture of crystalline silica, minerals, inorganic filler materials, organic resin and inorganic pigments. The binding resin is usually polyester and 5-15% by weight. Metal ions such as iron, manganese and titanium are present in pigments and constituent minerals.

Inhalational exposure to dust from artificial stone has been associated with a specific disease profile – notably, accelerated silicosis and scleroderma. The pathogenic mechanisms for silica-related disease are only partly understood, and in the case of artificial stone less so.

For regulatory and educational purposes, it has been assumed that the pathogenicity of artificial stone dust is wholly attributable to crystalline silica content. However, this may not be appropriate as artificial stone is a composite material, and certain constituents may exacerbate (or theoretically reduce) the effects of silica alone.

Enhanced toxicity of silica in combination with metals has been evidenced in some previous animal research and enhanced toxicity may explain the accelerated rate of lung disease development for artificial stone workers.

The first step in dust-induced pulmonary fibrosis leading to clinical silicosis is the interaction of the inhaled dust particles with lung macrophages, particularly alveolar macrophages. What happens inside the macrophage, especially the phagolysosome, then determines whether pro-inflammatory cytokines are released triggering fibrogenesis. The reactivity of artificial stone dust particles inside the phagolysosome has yet to be systematically examined and the role of resin and metal ions in the pro-inflammatory process is not understood.

## Aim:

This project seeks to reduce the incidence of artificial stone silicosis, *as a first step*, by a more systematic understanding of the role of organic binding resins and metals in artificial stone toxicology. Specifically, the project assesses the rate and extent of biosolubility in artificial lysosomal fluid, with which inhaled particles would come into contact after phagocytosis by alveolar and interstitial macrophages in the lung.

## Approach:

This was a laboratory-based study, utilising samples of artificial stone dust carefully comminuted from a wide range of authentic artificial stone products with variable amounts of resin and metals. The dust was initially analysed with respect to particle size, crystalline mineralogical components, organic content and elemental content.

Dust samples were then incubated with artificial lysosomal fluid (ALF, pH4.5) with gentle agitation at 37C for periods of up to 8 weeks. The metal ion concentrations in ALF were periodically analysed. Finally, the stone residue was recovered and organic content analysed to determine the extent of resin biosolubility.

## Findings and Interpretation:

### *Physicochemical data*

The main crystalline species for 25 samples, across 6 suppliers, were quartz and cristobalite with lesser amounts of albite, magnetite, rutile and hematite. The presence of the metals in 15 samples across 5 suppliers is generally consistent with information in the AS safety data sheets, including minerals such as rutile, magnetite, and hematite. In general, the darker coloured stones had more iron and manganese, and correlated with maximum iron and manganese metal ion release in ALF.

### *Organic resin biosolubility*

The average biosolubility after 8 weeks was 7%, ranging from 1-17%, across 14 samples from 5 suppliers.

This suggests that there is minor solubilisation of the resin in ALF. The conclusion about limited resin biosolubility is supported by scanning electron micrographs of two stones, before and after incubation with ALF, and calcination at 600C.

### *Metal ion biosolubility*

Ten samples from 5 suppliers demonstrated extensive biosolubility in ALF for iron (39-96%), and manganese (58-94%) even after one week. The biosolubility of aluminium and titanium in ALF was also significant, based on the amount that could be extracted by strong acid treatment, i.e. aluminium (40-100%) and titanium (46-86%). However, less than 10% of the aluminium and titanium was dissolved in ALF, based on the total amount of aluminium and titanium available. These data suggest that there are forms of iron and manganese (e.g. manganiferous iron ores) present in the artificial stones that are readily solubilised in ALF, probably via complexation with chelating agents, such as citrate, in ALF.

### *Rate of metal ion release*

Fourteen samples, from 5 suppliers, were incubated with ALF over 8 weeks. This study demonstrated substantial variability in potential metal ion release from AS dust in a simulated lung cell acidic environment. There were significant differences in metal ion release, depending on the AS type, particularly iron release. Time trends for metal release also varied with AS type but also metal ion. For most artificial stones the metal ion release was relatively rapid, with little further increase after the first week.

## Conclusions:

It is clear from this research that not all artificial stone products behave in the same way in artificial lysosomal fluid. The extent of resin solubilisation is minor, but not insignificant. Iron and manganese can be readily released, potentially exacerbating the effects of crystalline silica via catalytic formation of reactive oxygen species.

## Implications and Recommendations:

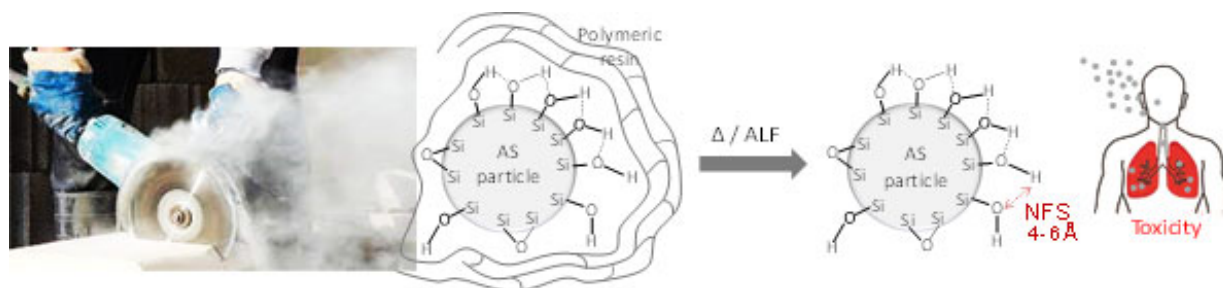
### The need for followup toxicology

With this new understanding of variable organic and inorganic content, biosolubility, and rates of metal ion release, *suitable followup toxicology experiments should be conducted*, perhaps using the data generated here as a guide to framing experimentation. Such experiments should use respirable dust and relevant lung cells, including macrophages and fibroblasts, as well as markers of inflammation and cytotoxicity.

Some research along these lines is about to commence with funding through the MRFF scheme, with Gaskin and Pisaniello as named investigators, and led by Prof. Graeme Zosky (University of Tasmania).

### Possible Trojan horse effect

Some early data from Italian collaborators (Drs Pavan and Turci, University of Turin) indicate that AS-induced phagolysosome membranolysis is not evident prior to incubation, but is, surprisingly, evident after the dust has been incubated with ALF for 8 weeks. This is evidence of the “Trojan horse” effect suggested in our original grant application, as well as by Pavan and Turci, whereby the resin is initially protective, but then exposes reactive silica surfaces.



Graphic – courtesy Pavan et al (unpublished)

*Further membranolysis experiments, with hemolysis assays, e.g. with samples generated as part of this MAQHSC-sponsored project, should be conducted.* This will increase our understanding of lung fibrogenesis, which constituents of artificial stone are most hazardous and clarify the role of the organic resin.

### Crystallinity is not a requirement for silica toxicity

The assumption of crystalline silica content being the only lung fibrosis risk factor is questionable. For one thing, pure synthetic quartz does not have hemolytic potential, but certain forms of amorphous silica do (e.g. vitreous silica). Thus, crystallinity is not an essential requirement for silica toxicity, but rather a particular surface configuration of (“nearly free”) silanol groups appears to be needed.

Relatedly, we don’t know whether low silica artificial stone products reduce risk in proportion to silica content, or at all. *Whether or not low silica products have lower propensity for lung damage should be investigated.*

### Potential development of a fibrogenicity benchmark for silica-bearing materials

With the wide array of artificial stone products on the market, there is a need to clarify not just the silica issue, but also the contribution of metals (e.g. from pigments) and organic resin towards lung disease.

*The development of an evidence-based benchmark for fibrogenicity should be developed.* This will allow hazards to be better understood and regulatory arrangements to be more nuanced. Such a benchmark would not just apply to artificial stone, but all silica-containing dust, e.g. in mining and quarrying. Collaborators in the abovementioned MRFF project (Dr Jack Auty) are trialling an assay incorporating an artificial phospholipid membrane model, which may be a promising benchmark, and a simplified alternative to the traditional red blood cell hemolysis assay, which is the current best indicator.

### **Other issues:**

In the course of this research, two other issues have emerged.

Firstly, and despite Codes of Practice, it is evident that *the issue of AS-contaminated recycled water in wet cutting processes needs further investigation.* Early data from 3 collected water samples indicate 96 – 165 mg/L of crystalline silica, and that only about 0.5 ml of the aerosolised water would need to be inhaled during the day to exceed the 0.05 mg/m<sup>3</sup> standard.

Secondly, a number of secondary exposures to airborne AS dust appear to be occurring and unregulated. This includes clean up and waste disposal procedures with no respiratory protection. Whilst the current thinking is that “aged” respirable dust may not be as reactive as freshly generated dust, there is limited empirical evidence that settled dust is less reactive. Longer term assays are required in the light of the potential Trojan horse effect mentioned above. *The issue of unprotected secondary exposures should be investigated.*

It should be noted that both of these issues have been identified from hygienists visiting workplaces, and collecting samples and making observations, in addition to normal exposure assessment. *An Occupational Hygiene Intelligence Network should be fostered to keep track of existing interventions and to identify any new issues.* This Network could be established under the auspices of SafeWork SA, and operate under Chatham House rules.

## 2. General Introduction

Artificial stone (AS), also known as engineered stone, is a composite material primarily used in kitchens and bathrooms as an alternative to granite and other natural stone. The exposure of workers breathing AS dusts during cutting, grinding, and abrasive polishing using power tools has been associated with accelerated silicosis, scleroderma, and upper respiratory diseases (Cooper et al, 2015; Leso et al, 2019; Fazen et al, 2020;)

A high prevalence of a new form of silicosis associated with extensive use of AS materials was first reported in Israel in 2006 (Ophir et al, 2019), following which, Spain, Italy, Australia, and United States have also reported cases of accelerated silicosis related to AS (Perez-Alonso et al, 2014; Hoy et al, 2018; Rose et al, 2019;

In addition to the increased incidence, epidemiological studies also suggest that the accelerated silicosis is associated with a comparatively rapid development of fibrosis, less exposure duration, a shorter latency period, and less visibility on X-ray and CT scan (Perez-Alonso et al, 2014; Paolucci et al, 2015).

Although there has been significant progress in reducing inhalation dust hazards in Australian workplaces, preventable occupational lung diseases such as silicosis have re-emerged (Hoy et al, 2018; Kirby 2019). There is uncertainty about the incidence and prevalence of accelerated silicosis in Australia, partly due to the absence of a national dust disease registry, and voluntary reporting by treating physicians. Voluntary notifications to the Thoracic Society of Australia and New Zealand's Occupational Lung Diseases Special Interest Group identified seven AS-associated silicosis cases between 2011 and 2016 (Hoy et al, 2018). The median age of those re-reported cases was 43 years, and the median duration of exposure was only 7.3 years, representing an accelerated disease development among young workers. A formal screening program in Queensland identified silicosis in more than 12% of AS workers, a much higher prevalence than normally expected for silica-exposed workers. Many of these workers were deemed to require lung transplants (Kirby, 2019).

The concerns about AS-associated silicosis and the comparatively young workers affected led to the development of the National Diseases Dust Taskforce in 2019 with the situation being viewed as a public health crisis (Australia Government Department of Health, undated).

In the case of AS, most benchtop fabricators are small businesses, and a lack of personal protective measures and engineering controls has been considered a plausible explanation for the occurrence of AS-related silicosis (Hoy et al, 2018; Leso et al, 2019).

Artificial stones are significantly different from natural stones and differing compositions could be related to higher toxicity (Leso et al, 2019). Apart from the high amount of crystalline silica, AS includes organic resin (typically, polyester 5-15% by weight), pigments, and other minerals such as feldspar (Madden et al, 2019).

The evidence relating to the toxicological and chemical properties of AS dust appears sparse, particularly the potential role played by resin and metal ions in the development of lung disease and broader immunological effects (Paolucci et al, 2015; Leso et al, 2019).

Elemental components such as metal ions are considered important contributors to lung toxicity, primarily due to their ability to produce reactive oxygen species (ROS) (Cohen 2004; Jaishankar et al, 2014).

Elements such as iron, chromium, and manganese may induce the overproduction of ROS causing oxidative stress leading to damage in cell components and ultimately cell malfunction

and death. The few studies that have assessed the chemical composition of respirable AS dust suggest that hetero ions present in AS dust are potentially responsible for higher toxicity and reactivity (Castranova et al, 1997; Paolucci et al, 2015; Pavan et al, 2016; Di Benedetto et al, 2019). Cohen (2004) reviewed the pulmonary toxicology of a range of metals, including aluminium and transition metals such as manganese. Changes have been noted in alveolar macrophages for manganese as  $MnCl_2$  and nickel as  $NiCl_2$ . More research is required, particularly for combinations of metals, for understanding intra-pulmonary effects (Cohen, 2004).

Element biosolubility studies are useful in assessing cell uptake evoking lung toxicity (Weggeberg et al, 2019). Simulated lung fluids simulating the interstitial and intracellular lung fluid environment have been used in several studies to assess the bioaccessibility of metallic constituents from vehicle dust, road exhaust, ultrafine airborne particulate matter, and high-temperature insulation wool (Colombo et al, 2008; Cannizzaro et al, 2019; Weggeberg et al, 2019).

With respect to artificial stone, the first step in pulmonary fibrosis, leading to clinical silicosis, is the interaction of the inhaled dust particles with lung macrophages, particularly alveolar macrophages. The macrophages engulf respirable size dust particles. What happens inside the macrophage, especially the phagolysosome, then determines whether pro-inflammatory cytokines are released triggering fibrogenesis. Dust component biosolubility is a major consideration. To date, the reactivity of artificial stone dust particles inside the phagolysosome has yet to be systematically examined and the role of resin and metal ions in the pro-inflammatory process is not understood.

To our knowledge, there are no reported biosolubility studies of AS metals or resin.

The current best predictor of pro-inflammatory activity for silica is hemolysis (Murashov et al, 2006; Pavan et al, 2014). The erythrocyte hemolysis assay is an indicator of whether the silica can cause membranolysis of the phagolysosome.

The assumption of crystalline silica content in airborne dust being the only lung fibrosis risk factor is questionable. For one thing, pure synthetic quartz does not have hemolytic potential, but certain forms of amorphous silica do (e.g. vitreous silica). Thus, crystallinity is not an essential requirement for silica toxicity, but rather a particular surface configuration of (“nearly free”) silanol groups appears to be needed (Pavan et al, 2020). If one starts with crystalline silica, the nearly free silanol groups may be generated by mechanical processes such as cutting, crushing and grinding the stone. Multiple crystal faces may be involved, leading to an irregular macroscopic fracture known as the *conchoidal* surface (Murashov et al, 2006). Such a fracture is visually similar to fractures that develop in vitreous silica.

Relatedly, we don’t know whether mechanical processing of low silica artificial stone products reduces risk in proportion to silica content, or at all. This may depend on how the silica was fractured. *Whether or not low silica products have a lower propensity for lung damage is unclear.*

For regulatory and educational purposes, it has been assumed that the pathogenicity of artificial stone dust is wholly attributable to crystalline silica content. However, this may not be appropriate as artificial stone is a composite material and AS fracture behaviour may be different from monolithic stones (Smolnicki et al, 2021).

Overall, there are knowledge gaps as to whether certain constituents may exacerbate (or theoretically reduce) the effects of silica alone.

## **Aim:**

This project seeks to reduce the incidence of artificial stone silicosis, *as a first step*, by a more systematic understanding of the role of organic binding resins and metals in artificial stone toxicology. Specifically, the project assesses the rate and extent of biosolubility in artificial lysosomal fluid, with which inhaled particles would come into contact after phagocytosis by alveolar and interstitial macrophages in the lung.

### **3. Initial characterisation & processing of artificial stone samples**

Authentic artificial stone samples were obtained from six different manufacturers (designated A-F), and were chosen on the basis of consumer popularity, colour and design. Each sample was initially cut using a wet diamond blade saw, and then crushed into small gravel-size pieces using a tungsten carbide jaw crusher in a specialized mineral processing facility in the University of Adelaide's School of Physical Sciences. These were further comminuted using a tungsten carbide ring mill for 4 minutes, maintaining moderate temperatures, to generate fine dust containing respirable and inhalable size particles.

Cross-contamination between samples was avoided by thoroughly cleaning the jaw-crusher and ring mill after and before each use. The handling of the comminuted ES was done in a fume cupboard as the dust was easily dispersed into the atmosphere. We used a real time aerosol photometer (*TSI DustTrak*) to identify and monitor dusty aspects of the work.

The following characteristics, except for organic resin, were determined by external NATA-accredited laboratories.

#### Size distribution of dust for selected stones

The mid-point of the size distribution was 10–18  $\mu\text{m}$ , as determined by wet sizing with a *Malvern Mastersizer 2000* (See **Appendix 1.1**).

#### Crystallographic analysis of selected stones

The main crystalline species for 25 samples, across 6 suppliers, were quartz and cristobalite with lesser amounts of albite, magnetite, rutile and hematite. (See **Appendix 1.2**)

#### Metal analyses of selected stones

Available metals (acid extractable) in the solid dust were determined by digestion with nitric and hydrochloric acid (1:1) for 1.5 h at 90–98 C prior to analysis by ICP-AES (atomic emission spectroscopy) and ICP-MS. The levels of practical quantification for Fe, Mn, Al and Ti, were 10, 1, 10 and 1 mg/kg.

Absolute metal content was determined by X-Ray Fluorescence.

See **Appendix 1.3** for metal content for 15 stones across 5 suppliers.

There was significant variability in metal content, especially for iron, manganese and titanium.

## Organic content of selected stones

The organic resin content for 25 stones across 6 suppliers was determined by weight loss after heating (calcination) to 600C, using a calibrated *Barnstead Thermolyne* muffle furnace with *CHY805 RTD* thermometer.

**Appendix 2** (column 1) shows a range of percent organic resin of 8.4% to 14.6%.

## Scanning electron microscopy (SEM)

See **Figure 1** below for a SEM image (back scattered electron mode) for one sample (BAS4). This image is consistent with the literature which describes a range of crystalline silica particle sizes being used in the production of artificial stone. The white particles are silica and the grey material is resin. The black background is carbon, used for SEM visualisation.

**Figure 2** (secondary electron mode) shows the topography and illustrates the rough surface associated with resin.



Figure 1: SEM (back scattered electron) image clearly illustrating crystalline silica embedded in, or attached to, resin.

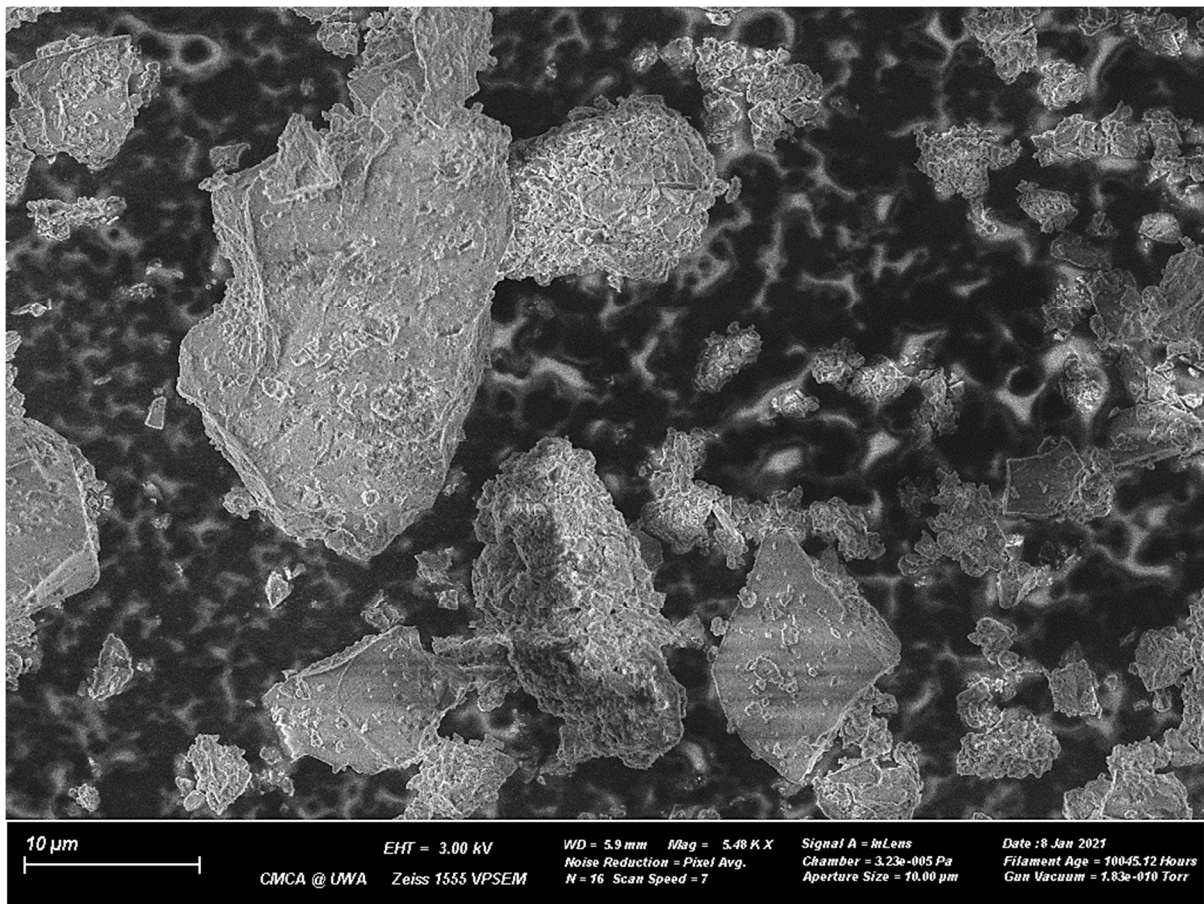


Figure 2: SEM (secondary electron) illustrating the topography of the particles in Figure 1.

## 4. Solubility Studies

### 4.1 Preparation of Artificial Lysosomal Fluid

Artificial lysosomal fluid (ALF) at pH 4.5, simulating the *in vivo* physiological condition of an acidic intracellular environment in lung cells, was used for the bioaccessibility investigations, as recommended by Pelfrène et al (2017). Gambles solution is an alternative, but this does not correspond to the pH conditions of the phagolysosome.

ALF was prepared following the composition used by Cannizzaro et al (2019). Analytical grade chemicals and ultra-pure water were used throughout to avoid contamination. ALF solution contains components such as pyruvate, citric acid, and glycine, which act as a growth media for many microorganisms; thus, 0.0002% formaldehyde was added to avoid microbial growth (Cannizzaro et al, 2019).

## 4.2 Organic Resin

### 4.2.1 Introduction

The detailed composition of the organic resin is not reported in safety data sheets for the artificial stones. In general, these are unsaturated polyester resins. **Appendix 2** shows the relative amounts of organic material in a range of artificial stone samples.

In order to establish the organic resin biosolubility, selected stones were reacted with ALF for 8 weeks and the organic content of the recovered solid material was determined. This was compared with the original content.

### 4.2.2 Methods

An accurately weighed quantity (5 g) of AS dust was mixed with 250 mL of ALF in a Schott bottle. The sealed bottles containing a mixture of AS dust and ALF were placed in a shaker (*Ratek OM25* orbital/mixer incubator) at 37C and gently agitated at 80 rpm.

After 8 weeks the supernatant liquid was carefully removed, and approximately 200 ml of pure water added. This was repeated two more times, and the solid residue dried at 60C overnight. This was re-weighed to determine the percentage recovery.

Approximately 95% of the original solid was recovered.

The recovered material was calcined at 600C (as above) to determine the organic content.

### 4.2.3 Results

**Appendix 2** shows that the average biosolubility after 8 weeks was 7%, ranging from 1-17%, across 14 samples from 5 suppliers.

This suggests that there is minor solubilisation of the resin in ALF for the particle size distributions mentioned above and in Appendix 1.1. The conclusion about limited resin biosolubility is supported by scanning electron micrographs of two stones, before and after incubation with ALF, and calcination at 600C.

**Figure 3** illustrates organic content loss with temperature, using a *Weatherford Laboratories Source Rock Analyser* with flame ionization detection. This indicates a similar type of organic resin, but larger quantities in the high resin stone.

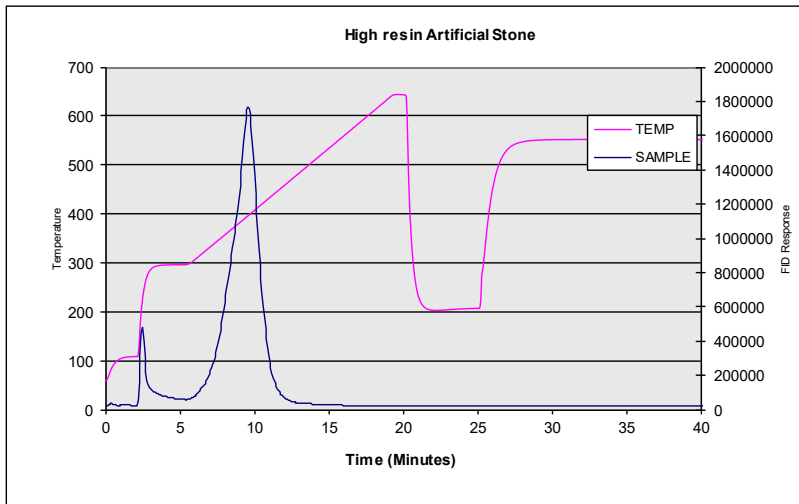
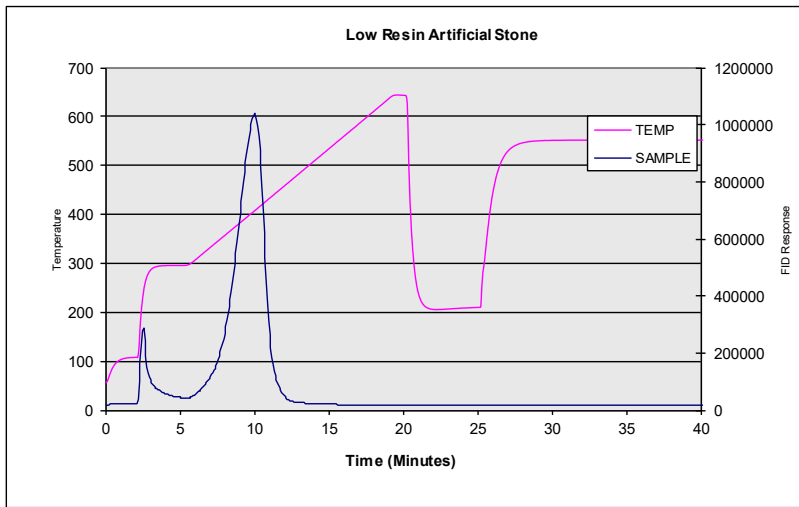


Figure 3: Pyrograms of low resin (left, sample BAS2) and high resin (right, sample BAS3) artificial stone.

#### 4.2.4 Interpretation

The variable biosolubility of organic resin is large (1-17%), only some of which may be attributable to experimental error. There may be subtle differences in the specific polyester formulation, which could render some formulations more susceptible to hydrolysis over extended periods. The implications of resin biosolubility remain to be explored, and toxicology experiments should be conducted with cured resin alone. There is some evidence of pulmonary inflammation from glass fibre-reinforced plastic containing unsaturated polyester resin (Abbate et al, 2006).

## 4.3 Metal Ions

### 4.3.1 Introduction

As mentioned, the release of metals ions from phagocytosed AS dust may have relevance to the development of fibrosis, via catalytic formation of reactive oxygen species (Fubini and Fenoglio, 2007). The objective was to determine the absolute amounts released and time trends, using a range of artificial stones from various suppliers.

### 4.3.2 Methods

Five grams of AS dust was mixed with 250 mL of ALF in a Schott bottle. The sealed bottles were placed on an orbital shaker at 37 C and gently agitated at 80 rpm. Thirty-millilitre aliquots of ALF fluid were then extracted periodically at one week, two weeks, four weeks and eight weeks of interaction, and filled again with 30 mL of new ALF. The pH was noted at all time points. A blank (250 mL ALF without any AS dust) was used for every batch as a quality control. The extracted 30 mL ALF aliquots were centrifuged in metal free centrifuge tubes at 4000 rpm for 15 min to settle any suspended particles if present. None of the aliquots had any visible residues at the bottom of the tube after centrifugation. The aliquots, including blanks, were forwarded to a commercial laboratory with a National Association of Testing Authorities accreditation to perform elemental analysis of metal ions such as iron (Fe), Manganese (Mn), Aluminum (Al) and Titanium (Ti). A standard method using inductively coupled plasma-mass spectrometry (ICP-MS) was used. Adjustments for dilution with fresh ALF were made in the reporting of metal ion concentrations. In initial experiments, a linear relationship was observed in metal ion concentrations for samples that had 1, 2, 4, and 10 g of solid. Thus, the values reported here are also normalized on a gram basis, i.e., concentrations are expressed as micrograms/litre per gram of solid.

### 4.3.3 Results

Fourteen AS dusts from five different companies (prefixes A–E) were assessed for metal ion release in ALF. **Appendix 3** provides the tabulated data of metal ion concentrations by time point.

Although 12 elements were determined, based on likely content in the AS, only four elements, aluminium, titanium, manganese, and iron are included here as the metal ion concentration of vanadium, arsenic, nickel, copper, chromium, and antimony were at or below the limit of detection. For Fe, Mn, Al and Ti, these were 10, 5, 10 and 1 µg/L for liquid samples.

In addition, tungsten and cobalt were not included as these could be introduced as contaminants during stone dust generation using tungsten carbide (Yamasaki, 2018).

There were significant differences in the release of Fe, Al, Mn and Ti, depending on the stone type. These tend to reflect the metal amounts inherent in the dust.

## **Amount and rate of metal ion release**

### Iron

There is significant variability in absolute terms. As can be seen from Appendix 3 Table A3.1, AAS1 had the highest value of Fe release and the values increased steadily from week 1 to week 8. It is interesting that this sample had 0.8% crystalline magnetite as determined by quantitative X-ray diffraction, and that the dust can be attracted to a strong magnet. However, Fe release remained similar from week 1 and week 8 for other AS samples (except BAS2). These data suggest that iron is solubilised relatively rapidly.

### Aluminium

Aluminium was found to be a relatively abundant element released in ALF, which is to be expected as AS typically contains aluminosilicate minerals, such as feldspars. Table A3.3 shows moderate variability in absolute terms.

### Manganese and Titanium

Table A3.2 shows that there is significant variability in the manganese release in absolute terms, but the time trend is relatively flat. Table A3.4 shows less variability for titanium in absolute terms and similar flatness in terms of time trend. Titanium can be present as titanium dioxide (rutile), used as a white pigment.

## **Metal ion biosolubility**

The proportion of metal released, relative to the amount available as acid extractable metal, was calculated as (maximum metal ion concentration ( $\mu\text{g/L}$ )  $\times$  0.25 L)/available metal in the dust ( $\mu\text{g/g}$ ).

Ten samples from 5 suppliers demonstrated extensive biosolubility in ALF for iron (39-96%), and manganese (58-94%) even after one week. The biosolubility of aluminium and titanium in ALF was also significant, based on the amount that could be extracted by strong acid treatment, i.e. aluminium (40-100%) and titanium (46-86%). However, less than 10% of the aluminium and titanium was dissolved in ALF, based on the total amount of aluminium and titanium available, as assessed by XRF (Appendix 1.3).

In general, the darker coloured stones had more iron and manganese, and correlated with maximum iron and manganese metal ion release in ALF.

## **4.3.4 Interpretation**

These data suggest that there are forms of iron and manganese (e.g. manganiferous iron ores) present in the artificial stones that are readily solubilised in ALF, probably via complexation with chelating agents in ALF, such as citrate (Gautier-luneau et al, 2007).

## 5. General Discussion

### Organic resin

This is the first study reporting organic resin “biosolubility” in ALF. It is likely that the resin simply breaks down by hydrolysis and the smaller molecules are incorporated into the supernatant liquid. The ester hydrolysis may result in ester carbonyl functionality being converted to carboxylic acid and hydroxyl functional groups (Visco et al 2012). Further research is needed to identify the breakdown products.

### Metal ions

This is the first study reporting AS metal ion release in ALF. The data indicate extensive, and sometimes progressive, metal solubilization in acid environments (pH 4.5) corresponding to the intracellular environment of lung macrophage lysosomes. This is possibly due to chelation of the metals, driving the equilibrium towards soluble metal-organic moieties.

The presence of the metals is generally consistent with information in the safety data sheet (SDS) for the AS, including minerals such as rutile, magnetite, and hematite (Madden et al, 2019). However, the information in SDSs is limited and does not provide proportionate information on iron or any other elemental constituents. In addition, the SDS are usually not specific for a stone type. Thus, the users of the products are unaware of the amounts of metals in the base minerals or pigments.

The source of various metals could be the mineral constituents, pigments, organic resins, and stone processing activities. Precise information on minerals, pigments and resins used for AS manufacture is commercially sensitive and the elements could vary depending on the source of raw materials used. A source of Fe and Mn could possibly be the inorganic pigments. Titanium could be due to rutile, giving a white appearance. The stone processing activities in industrial stone workshops may introduce different elements such as Co, W and Fe (Di Benedetto et al, 2019; Yamasaki, 2018). For example, Co and W could be introduced through cutting and grinding of AS slabs using tungsten carbide. A study comparing parent and processed ES dust found that there can be significant chemical variability between parent and processed dust. The variation was found to relate to the type of processing such as dry cutting or wet cutting (Di Benedetto et al, 2019). Another source of element contamination in AS is the polyester resin binder, although the amount of metal catalyst is very small (Jansen et al, 2013).

Metals assessed in this study may enhance lung toxicity from crystalline silica (Castranova et al, 1997; Hetland et al, 2000; Becher et al, 2001). Manganese and iron are essential cations for cell function in trace amounts. However, where there is imbalance, these are toxicogenic and damage lung cells and tissues (Neves et al, 2019). The presence of excessive Fe and Mn may enhance production of reactive oxygen species (ROS), converting hydrogen peroxide into very reactive hydroxyl species, resulting in cell damage (Martinez-Finley et al, 2013; Fubini and Fenoglio, 2007).

## Limitations

There are a number of limitations in this project.

The metal ions were not speciated. The ability of ferrous ion to participate in the Fenton reaction (producing reactive oxygen species) is much greater than the ferric ion (Zosky et al, 2021).

Only one batch of each sample was analysed. There may be slightly different silica, mineral, metal and resin content in different commercial batches, owing to the availability and variability of raw materials.

The biosolubility may vary by particle size. This may be particularly relevant for organic resin, as one would expect hydrolysis would be more efficient with smaller sized particles.

The mineral particle sizes in the original slab were not determined. However, it is known that a range of particle sizes of materials are in artificial stone slab production (Lee et al, 2008)

## 6. Implications and Recommendations

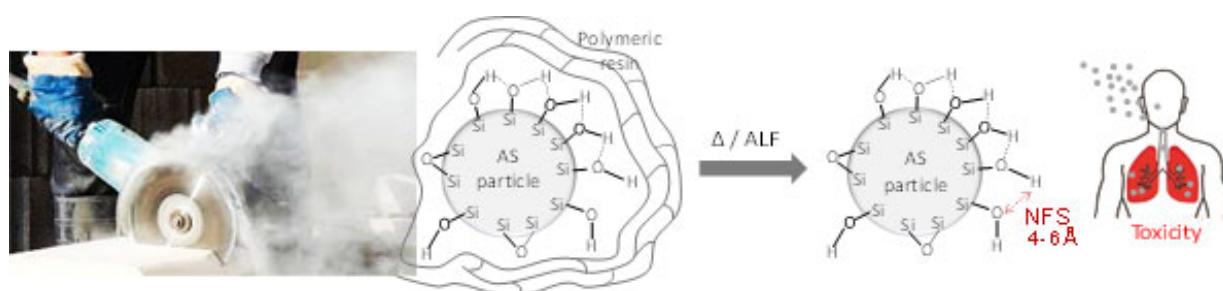
### The need for followup toxicology

With this new understanding of variable organic and inorganic content, biosolubility, and rates of metal ion release, *suitable followup toxicology experiments should be conducted*, perhaps using the data generated here as a guide to framing experimentation. Such experiments should use respirable dust and relevant lung cells, including macrophages and fibroblasts, as well as markers of inflammation and cytotoxicity.

Some research along these lines is about to commence with funding through the MRFF scheme, with Gaskin and Pisaniello as named investigators, and led by Prof. Graeme Zosky (University of Tasmania).

### Possible Trojan horse effect

Some early data from Italian collaborators (Drs Pavan and Turci, University of Turin) indicate that AS-induced phagolysosome membranolysis is not evident prior to incubation, but is, surprisingly, evident after the dust has been incubated with ALF for 8 weeks. This is evidence of the “Trojan horse” effect suggested in our original grant application, as well as by Pavan and Turci, whereby the resin is initially protective, but then exposes reactive silica surfaces.



Graphic – courtesy Pavan et al (unpublished)

*Further membranolysis experiments, with hemolysis assays, e.g. with samples generated as part of this MAQOHSC-sponsored project, should be conducted.* This will increase our

understanding of lung fibrogenesis, which constituents of artificial stone are most hazardous and clarify the role of the organic resin.

#### Crystallinity is not a requirement for silica toxicity

The assumption of crystalline silica content being the only lung fibrosis risk factor is questionable. For one thing, pure synthetic quartz does not have hemolytic potential, but certain forms of amorphous silica do (e.g. vitreous silica). Thus, crystallinity is not an essential requirement for silica toxicity, but rather a particular surface configuration of (“nearly free”) silanol groups appears to be needed (Pavan et al, 2020).

Relatedly, we don’t know whether low silica artificial stone products reduce risk in proportion to silica content, or at all. *Whether or not low silica products have lower propensity for lung damage should be investigated.*

#### Potential development of a fibrogenicity benchmark for silica-bearing materials

With the wide array of artificial stone products on the market, there is a need to clarify not just the silica issue, but also the contribution of metals (e.g. from pigments) and organic resin towards lung disease.

*The development of an evidence-based benchmark for fibrogenicity should be developed.* This will allow hazards to be better understood and regulatory arrangements to be more nuanced. Such a benchmark would not just apply to artificial stone, but all silica-containing dust, e.g. in mining and quarrying. Collaborators in the abovementioned MRFF project (Dr Jack Auty) are trialling an assay incorporating an artificial phospholipid membrane model, which may be a promising benchmark, and a simplified alternative to the traditional red blood cell hemolysis assay, which is the current best indicator.

#### **Other issues:**

In the course of this research, two other issues have emerged.

Firstly, and despite Codes of Practice, it is evident that *the issue of AS-contaminated recycled water in wet cutting processes needs further investigation.* Early data from 3 collected water samples suggest 96 – 165 mg/L of crystalline silica, and that only about 0.5 ml of the aerosolised water would need to be inhaled during the day to exceed the 0.05 mg/m<sup>3</sup> standard.

Secondly, a number of secondary exposures to airborne AS dust appear to be occurring and unregulated. This includes clean up and waste disposal procedures with no respiratory protection. Whilst the current thinking is that “aged” respirable dust may not be as reactive as freshly generated dust, there is limited empirical evidence that settled dust is less reactive. Longer term assays are required in the light of the potential Trojan horse effect mentioned above. *The issue of unprotected secondary exposures should be investigated.*

It should be noted that both of these issues have been identified from hygienists visiting workplaces, and collecting samples and making observations, in addition to normal exposure assessment. *An Occupational Hygiene Intelligence Network should be fostered to keep track of existing interventions and to identify any new issues.* This Network could be established under the auspices of SafeWork SA, and operate under Chatham House rules.

## 7. Acknowledgements

Firstly, we wish to thank the SA Mining and Quarrying Occupational Health and Safety Committee for financial support of the project.

We would like to thank Dr Joseph Crea, Dr Michael Tkaczuk, Ms Preeti Maharjan and Dr Chandnee Ramkissoon for assistance with laboratory experimentation, and Dr Laurie Glossop with assistance with scanning electron microscopy.

We also acknowledge the assistance of Dr Tony Hall and Dr Fionnuala Sheehan from the School of Physical Sciences, University of Adelaide, for assistance with selected XRD analyses, pyrograms and sample comminution. Finally, we thank Shelley Rowett (SafeWork SA) for critical comments and HSE Australia for assistance with calcination of selected samples.

## 8. References

Abbate, C.; Giorgianni, C.; Brecciaroli, R.; Giacobbe, G.; Costa, C.; Cavallari, V.; Albiero, F.; Catania, S.; Tringali, M.A.; Martino, L.B.; Abbate, S. Changes Induced by Exposure of the Human Lung to Glass Fiber-Reinforced Plastic. *Environ Health Perspect.* 2006, 114, 1725–1729. doi:10.1289/ehp.8676

Australia Government Department of Health. National Dust Disease Taskforce. Available online: <https://www1.health.gov.au/internet/main/publishing.nsf/Content/ohp-nat-dust-disease-taskforce.htm>

Becher, R.; Hetland, R.B.; Refsnes, M.; Dahl, J.E.; Dahlman, H.J.; Schwarze, P.E. Rat Lung Inflammatory Responses after In Vivo and In Vitro Exposure to Various Stone Particles. *Inhal. Toxicol.* 2001, 13, 789–805, doi:10.1080/08958370118221.

Cannizzaro, A.; Angelosanto, F.; Barrese, E.; Campopiano, A. Biosolubility of High Temperature Insulation Wools in Simulated Lung Fluids. *J. Occup. Med. Toxicol.* 2019, 14, 15, doi:10.1186/s12995-019-0235-z.

Castranova, V.; Vallyathan, V.; Ramsey, D.M.; McLaurin, J.L.; Pack, D.; Leonard, S.; Barger, M.W.; Ma, J.Y.; Dalal, N.S.; Teass, A. Augmentation of Pulmonary Reactions to Quartz Inhalation by Trace Amounts of Iron-Containing Particles. *Environ. Health Perspect.* 1997, 105 (Suppl 5), 1319–1324, doi:10.1289/ehp.97105s51319.

Cohen, M. Pulmonary Immunotoxicology of Select Metals: Aluminum, Arsenic, Cadmium, Chromium, Copper, Manganese, Nickel, Vanadium, and Zinc. *J. Immunotoxicol.* 2004, 1, 39–69, doi:10.1080/15476910490438360.

Colombo, C.; Monhemius, A.J.; Plant, J.A. Platinum, Palladium and Rhodium Release from Vehicle Exhaust Catalysts and Road Dust Exposed to Simulated Lung Fluids. *Ecotoxicol. Environ. Saf.* 2008, 71, 722–730, doi:10.1016/j.ecoenv.2007.11.011.

Cooper, J.H.; Johnson, D.L.; Phillips, M.L. Respirable Silica Dust Suppression during Artificial Stone Countertop Cutting. *Ann. Occup. Hyg.* 2015, 59, 122–126, doi:10.1093/annhyg/meu083.

Di Benedetto, F.; Giaccherini, A.; Montegrossi, G.; Pardi, L.A.; Zoleo, A.; Capolupo, F.; Innocenti, M.; Lepore, G.O.; d’Acapito, F.; Capacci, F.; et al. Chemical Variability of Artificial

- Stone Powders in Relation to their Health Effects. *Sci. Rep.* 2019, 9, 6531, doi:10.1038/s41598-019-42238-2.
- Fazen, L.E.; Linde, B.; Redlich, C.A. Occupational Lung Diseases in the 21st Century: The Changing Landscape and Future Challenges. *Curr. Opin. Pulmon. Med.* 2020, 26, 142–148.
- Fubini, F.; Fenoglio, I. Toxic Potential of Mineral Dusts. *Elements* 2007, 3, 407–414, doi:10.2113/GSELEMENTS.3.6.407.
- Gautier-luneau, I.; Bertet, P.; Jeunet, A.; Serratrice, G.; Pierre, J.L. Iron-citrate Complexes and Free Radicals Generation: Is Citric Acid an Innocent Additive in Foods and Drinks?. *Biometals* 2007, 20, 793–796. doi:10.1007/s10534-006-9042-y
- Hetland, R.B.; Refsnes, M.; Myran, T.; Johansen, B.V.; Uthus, N.; Schwarze, P.E. Mineral and/or Metal Content as Critical Determinants of Particle-Induced release of IL-6 and IL-8 from A549 cells. *J. Toxicol Environ. Health A* 2000, 60, 47–65, doi:10.1080/009841000156583.
- Hoy, R.F.; Baird, T.; Hammerschlag, G.; Hart, D.; Johnson, A.R.; King, P.; Putt, M.; Yates, D.H. Artificial Stone-Associated Silicosis: A Rapidly Emerging Occupational Lung Disease. *Occup. Environ. Med.* 2018, 75, 3–5, doi:10.1136/oemed-2017-104428.
- Jaishankar, M.; Tseten, T.; Anbalagan, N.; Mathew, B.B.; Beeregowda, K.N. Toxicity, Mechanism and Health Effects of Some Heavy Metals. *Interdiscip. Toxicol.* 2014, 7, 60–72, doi:10.2478/intox-2014-0009.
- Jansen, J.F.G.A.; Hilker, I.; Kleuskens, E.; Hensen, G.; Kraeger, I.; Posthumus, W. Cobalt Replacement in Unsaturated Poly-ester Resins-Going for Sustainable Composites. *Macromol. Symp.* 2013, 329, 142–149, doi:10.1002/masy.201200102.
- Kirby, T. Australia Reports on Audit of Silicosis for Stonecutters. *Lancet* 2019, 393, 861, doi:10.1016/S0140-6736(19)30478-7.
- Lee, M.; Ko, C.; Chang, F.; Lo, S.; Lin, J.; Shan, M.; Lee, J. Artificial Stone Slab Production Using Waste Glass, Stone Fragments and Vacuum Vibratory Compaction. *Cement & Concrete Composites.* 2008 30, 583-587. doi: 10.1016/j.cemconcomp.2008.03.004
- Leso, V.; Fontana, L.; Romano, R.; Gervetti, P.; Iavicoli, I. Artificial Stone Associated Silicosis: A Systematic Review. *Int. J. Environ. Res. Public Health* 2019, 16, 568, doi:10.3390/ijerph16040568.
- Madden, C.; Davidson, M.; O'Donnell, G.; Reed, S. Characterisation of Respiratory Hazards during the Manufacture and Installation of Engineered and Natural Stone Products. In *Proceedings of the 37th Annual Conference and Exhibition, Perth, Australia, 20 November–4 December 2019*; pp. 55–64, ISBN: 978-0-9577703-6-2. Available online: <https://www.aioh.org.au/static/uploads/files/aioh-2019-conference-proceedings-combined-file-v2-wfxyrwknmls.pdf>
- Martinez-Finley, E.J.; Gavin, C.E.; Aschner, M.; Gunter, T.E. Manganese Neurotoxicity and the Role of Reactive Oxygen Spe-cies. *Free Rad. Biol. Med.* 2013, 62, 65–75, doi:10.1016/j.freeradbiomed.2013.01.032.

Murashov, V.; Harper, M.; Demchuk, E. Impact of Silanol Surface Density on the Toxicity of Silica Aerosols Measured by Erythrocyte Haemolysis, *J. Occup. Environ. Hyg.* 2006, 3, 718–723, doi:10.1080/15459620601015950.

Neves, J.; Haider, T.; Gassmann, M.; Muckenthaler, M.U. Iron Homeostasis in the Lungs-A Balance between Health and Disease. *Pharmaceuticals* 2019, 12, 5, doi:10.3390/ph12010005.

Ophir, N.; Amir Bar, S.; Korenstein, R.; Kramer, M.R.; Fireman, E. Functional, Inflammatory and Interstitial Impairment due to Artificial Stone Dust Ultrafine Particles Exposure. *Occup. Environ. Med.* 2019, 76, 875–879, doi:10.1136/oemed-2019-105711.

Paolucci, V.; Romeo, R.; Sisinni, A.G.; Bartoli, D.; Mazzei, M.A.; Sartorelli, P. Silicosis in Workers Exposed to Artificial Quartz Conglomerates: Does it Differ from Chronic Simple Silicosis? *Arch. Bronconeumol.* 2015, 51, e57–e60, doi:10.1016/j.arbres.2014.12.010.

Pavan, C.; Polimeni, M.; Tomatis, M.; Corazzari, I.; Turci, F.; Ghigo, D.; Funini, B. Abrasion of Artificial Stones as a New Cause of an Ancient Disease. Physicochemical Features and Cellular Responses. *Toxicol. Sci.* 2016, 153, 4–17, doi:10.1093/toxsci/kfw101.

Pavan, C.; Rabolli, V.; Tomatis, M.; Fubini, B.; Lison, L. Why Does the Hemolytic Activity of Silica Predict its Pro-Inflammatory Activity? *Part. Fib. Toxicol.* 2014 11,76, doi: 10.1186/s12989-014-0076-y

Pavan, C.; Santalucia, R.; Leinardi, R.; Fabbiani, M.; Yakoub, Y.; Uwambayinema, F.; Ugliengo, P.; Tomatis, M.; Martra, G.; Turci, F.; et al. Nearly Free Surface Silanols are the Critical Molecular Moieties that Initiate the Toxicity of Silica Particles. *Proc. Natl. Acad. Sci. USA* 2020, 117, 27836–27846, doi:10.1073/pnas.2008006117.

Pelfrène, A.; Cave, M.R.; Wragg, J.; Douay, F. In Vitro Investigations of Human Bioaccessibility from Reference Materials using Simulated Lung Fluids. *Int. J. Environ. Res Public Health* 2017, 14, 112, doi:10.3390/ijerph14020112.

Perez-Alonso, A.; Cordoba-Dona, J.A.; Millares-Lorenzo, J.L.; Figueroa-Murillo, E.; Garcia-Vadillo, C.; Romero-Morillos, J. Outbreak of Silicosis in Spanish Quartz Conglomerate Workers. *Int. J. Occup. Environ. Health* 2014, 20, 26–32, doi:10.1179/2049396713Y.0000000049.

Rose, C.; Heinzerling, A.; Patel, K.; Sack, C.; Wolff, J.; Zell-Baran, L.; Weissman, D.; Hall, E.; Sooriash, R.; McCarthy, R.B.; et al. Severe Silicosis in Engineered Stone Fabrication Workers-California, Colorado, Texas, and Washington, 2017–2019. *MMWR Morb. Mortal. Wkly. Rep.* 2019, 68, 813–818, doi:10.15585/mmwr.mm6838a1.

Smolnicki, M.; Cieciora, M.; Lesiuk, G.; Correia, J.; Stabla, P. Fracture Behaviour of Engineering Stone Material, *Int. J. Struct. Integrity.* 2021, 12(1), 70-88. doi:10.1108/IJSI-05-2019-0047

Visco, A.; Brancato, V.; Campo, N. Degradation Effects in Polyester and Vinyl Ester Resins Induced by Accelerated Aging in Seawater. *J. Comp. Mat.* 2012 46(17), 2025–2040. doi: 10.1177/0021998311428533

Weggeberg, H.; Benden, T.F.; Steinnes, E.; Flaten, T.P. Element Analysis and Bioaccessibility Assessment of Ultrafine Air-borne Particulate Matter (PM<sub>0.1</sub>) Using Simulated Lung Fluid Extraction (Artificial Lysosomal Fluid and Gamble's Solution). *Environ. Chem. Ecotoxicol.* 2019, 1, 26–35, doi:10.1016/j.eneco.2019.08.001.

Yamasaki, T. Contamination from Mortars and Mills during Laboratory Crushing and Pulverizing. *Bull. Geol. Surv. Jpn.* 2018; 69, 201–210.

Zosky, G.R.; Bennett E.J.; Pavez, M.; Beamish, B.B. No Association Between Pyrite Content and Lung Cell Responses to Coal Particles. *Sci Rep.* 2021 Apr 14;11(1):8193. doi: 10.1038/s41598-021-87517-z.

## **9 Appendices**

**Appendix 1: Physicochemical characterisation of comminuted artificial stones**

**Appendix 1.1: Wet sizing of selected comminuted artificial stones**

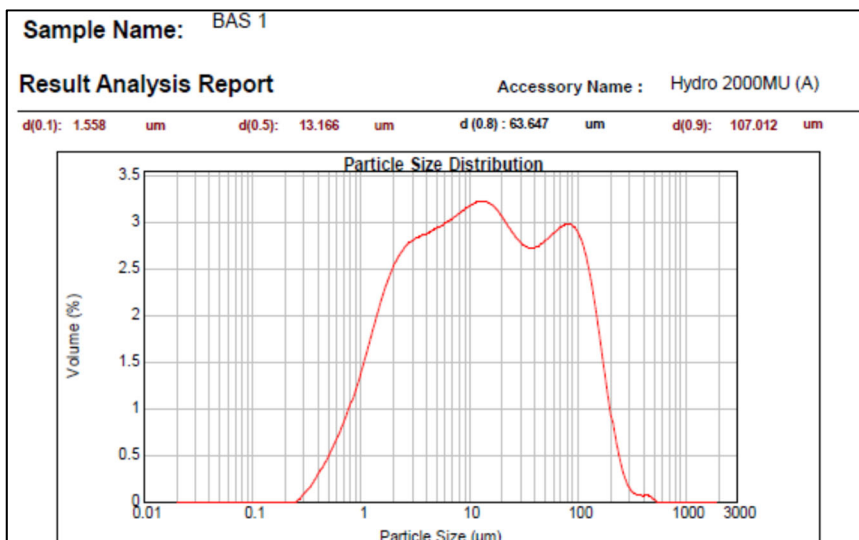
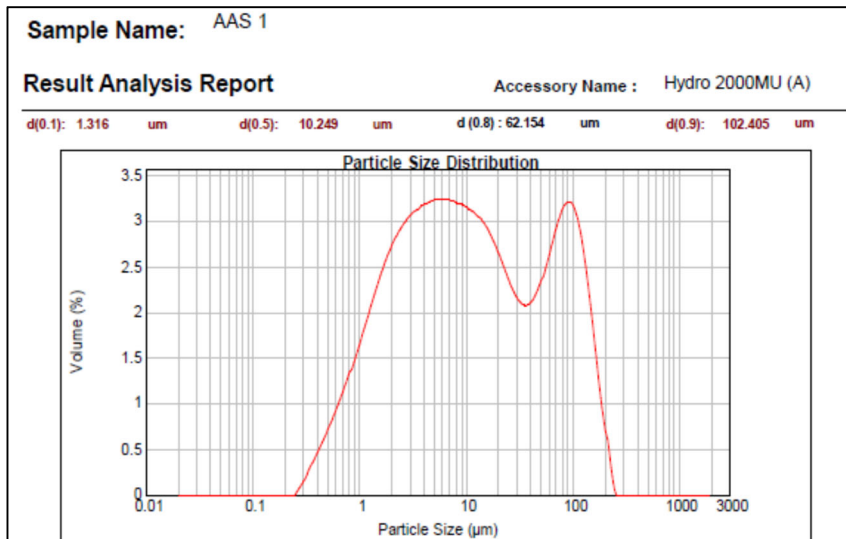
**Appendix 1.2: Mineralogical analyses of comminuted artificial stones**

**Appendix 1.3: Elemental analyses of comminuted artificial stones**

**Appendix 2: Organic analyses of selected comminuted artificial stones**

**Appendix 3: Time trends of metal ion release in ALF**

## Appendix 1.1: Wet sizing of selected comminuted artificial stones

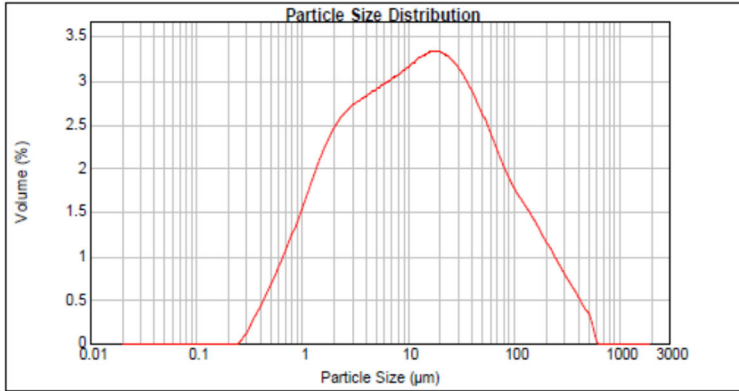


Sample Name: BAS 2

Result Analysis Report

Accessory Name : Hydro 2000MU (A)

d(0.1): 1.388 um      d(0.5): 12.536 um      d(0.8): 54.724 um      d(0.9): 115.248 um

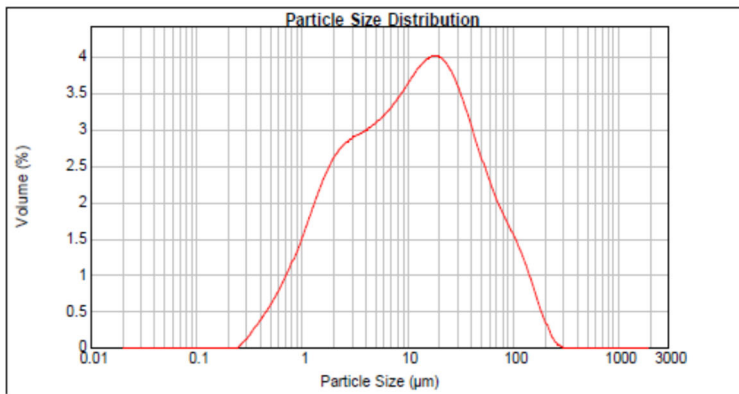


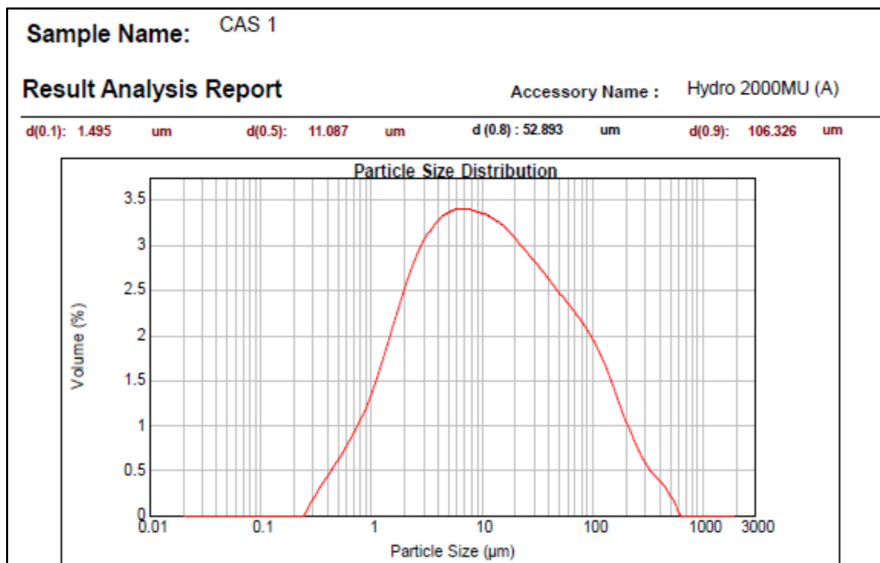
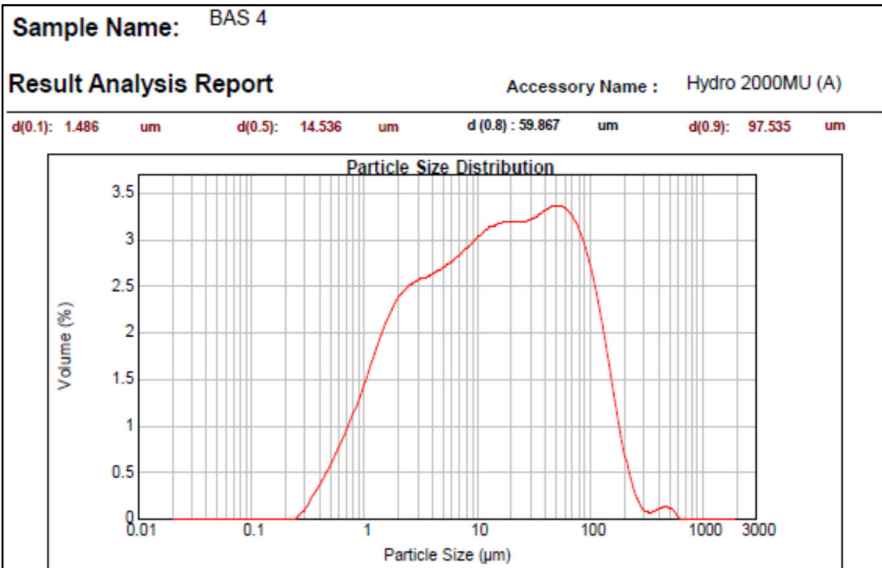
Sample Name: BAS3

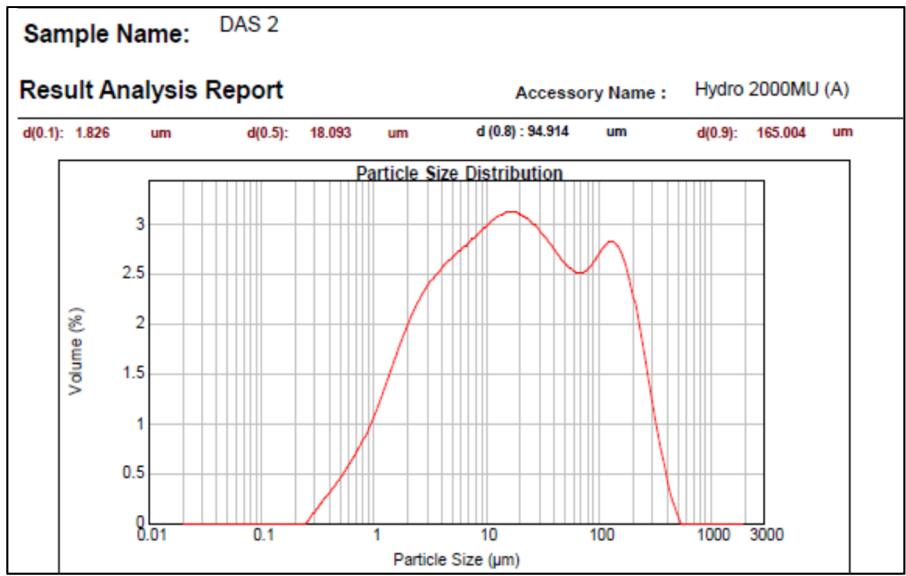
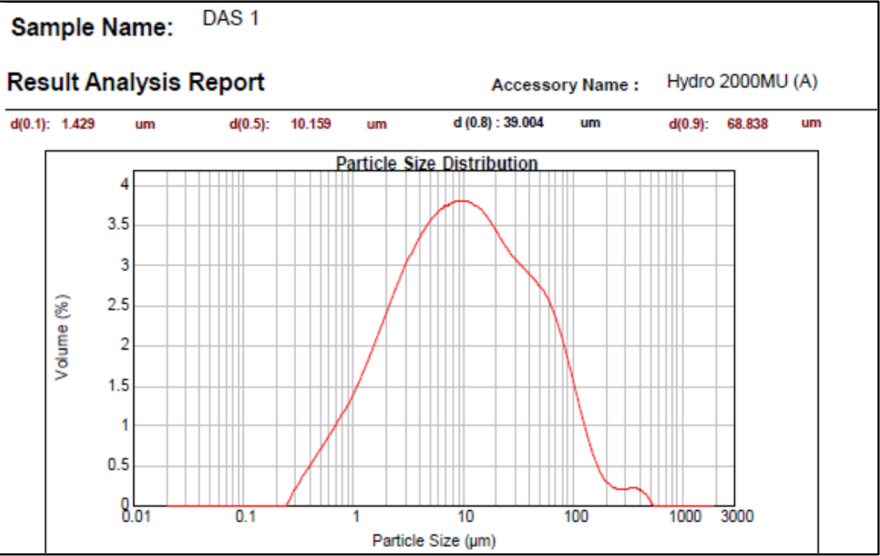
Result Analysis Report

Accessory Name : Hydro 2000MU (A)

d(0.1): 1.438 um      d(0.5): 11.131 um      d(0.8): 37.102 um      d(0.9): 65.777 um







## Appendix 1.2: Mineralogical analyses of comminuted artificial stones

Main crystalline species (weight percent)\*

| Stone Type | Quartz<br>Wt % | Cristobalite<br>Wt % | Albite<br>Wt % | Hematite<br>Wt % | Rutile<br>Wt % | Magnetite<br>Wt % |
|------------|----------------|----------------------|----------------|------------------|----------------|-------------------|
| AAS1       | 89             | 0.4                  | 3.0            | 0.2              | n.d            | 0.8               |
| AAS2#      | 59             | 25                   | 10             | n.d.             | 5.6            | n.d.              |
| AAS3#      | 98             | n.d.                 | 0.2            | n.d              | 1.6            | n.d.              |
| AAS4#      | 96             | n.d.                 | 0.5            | n.d.             | 4              | n.d.              |
| AAS5#      | 94             | n.d.                 | 6.2            | n.d.             | n.d.           | n.d.              |
| AAS6#      | 99             | n.d.                 | 0.03           | n.d.             | 0.9            | n.d.              |
| AAS7#^     | 90             | n.d.                 | 6.9            | n.d.             | 2.0            | n.d.              |
| AAS8#      | 98             | n.d.                 | 1              | n.d.             | 0.4            | n.d.              |
| BAS1       | 56             | 24                   | 2.2            | n.d.             | 0.7            | n.d.              |
| BAS2       | 92             | n.d                  | n.d            | 0.4              | n.d.           | n.d.              |
| BAS3       | 19             | 47                   | 6              | n.d.             | 0.8            | n.d.              |
| BAS4       | 23             | 43                   | 7.2            | n.d.             | 0.5            | n.d.              |

|              |    |      |      |      |      |      |
|--------------|----|------|------|------|------|------|
| <b>BAS5#</b> | 70 | 30   | 0.2  | n.d. | n.d. | n.d. |
| <b>BAS6#</b> | 92 | n.d. | 7.3  | n.d. | 0.5  | n.d. |
| <b>BAS7#</b> | 65 | 24   | 11.4 | n.d. | n.d. | n.d. |
| <b>BAS8#</b> | 98 | n.d. | n.d. | n.d. | 1.9  | n.d. |
| <b>CAS1#</b> | 98 | n.d. | n.d. | n.d. | 1.8  | n.d. |
| <b>CAS2</b>  | 96 | n.d. | n.d. | n.d. | 4    | n.d. |
| <b>DAS1</b>  | 90 | 0.3  | n.d. | 0.1  | n.d. | 0.2  |
| <b>DAS2#</b> | 76 | 23   | n.d. | n.d. | 0.6  | n.d. |
| <b>EAS1</b>  | 99 | n.d. | n.d. | n.d. | n.d. | n.d. |
| <b>EAS2</b>  | 99 | n.d. | n.d. | n.d. | n.d. | n.d. |
| <b>EAS3#</b> | 99 | n.d. | n.d. | n.d. | n.d. | 0.01 |
| <b>FAS1#</b> | 10 | 90   | n.d. | n.d. | n.d. | n.d. |
| <b>FAS2#</b> | 78 | 16   | n.d. | n.d. | 5.6  | n.d. |
|              |    |      |      |      |      |      |

\*determined by X Ray Diffraction; n.d. not detected; #semi-quantitative: ^1.4% talc

Amorphous content of the artificial stones varied between 6.5% and 27%. The amorphous content of the stones is most likely due to a combination of polymer resin and amorphous silica (glass) material.

### Appendix 1.3: Elemental analyses of comminuted artificial stones

Acid extractable metal content and total metal content in dust

| Stone Type | Acid extractable Fe (mg/kg) | Total content XRF <sup>1</sup> (mg/kg) | Iron by Mn (mg/kg) | Acid extractable Mn (mg/kg) | Total Manganese content by XRF (mg/kg) | Acid extractable Al (mg/kg) | Total Aluminium content by XRF (mg/kg) | Acid extractable Ti (mg/kg) | Total Titanium content by XRF (mg/kg) |
|------------|-----------------------------|--|--------------------|-----------------------------|--|-----------------------------|--|-----------------------------|---------------------------------------|
| AAS1       | 3800                        | 5200                                   | 63                 | 77                          | 150                                    | 3150                        | 9                                      | 84                          |                                       |
| BAS1       | 40                          | <50                                    | 1                  | <10                         | 230                                    | 2570                        | 7                                      | 2930                        |                                       |
| BAS2       | 710                         | 756                                    | 23                 | <30                         | 250                                    | 2050                        | 4                                      | 252                         |                                       |
| BAS3       | 90                          | 110                                    | 7                  | <10                         | 160                                    | 4650                        | 7                                      | 3490                        |                                       |
| BAS4       | 50                          | 105                                    | 3                  | <10                         | 190                                    | 7160                        | 6                                      | 1880                        |                                       |
| BAS5       | 60                          | 200                                    | <1                 | n.d.                        | 140                                    | 2860                        | 3                                      | 600                         |                                       |
| BAS6       | 60                          | n.a.                                   | 2                  | n.d.                        | 330                                    | n.a.                        | 4                                      | n.a.                        |                                       |
| BAS7       | 40                          | n.a.                                   | 2                  | n.d.                        | 510                                    | n.a.                        | 19                                     | n.a.                        |                                       |
| CAS1       | 50                          | <100                                   | 3                  | n.d.                        | 330                                    | 1480                        | 6                                      | 2220                        |                                       |
| CAS2       | 40                          | 200                                    | 2                  | n.d.                        | 400                                    | 4030                        | 10                                     | 5460                        |                                       |
| DAS1       | 565                         | 880                                    | 21                 | 24                          | 140                                    | 2290                        | 8                                      | 780                         |                                       |
| DAS2       | 80                          | 200                                    | 3                  | n.d.                        | 60                                     | 1325                        | 7                                      | 1500                        |                                       |
| EAS1       | 100                         | 600                                    | 3                  | n.d.                        | 110                                    | 1380                        | <1                                     | 240                         |                                       |

|             |      |      |    |      |     |      |   |      |
|-------------|------|------|----|------|-----|------|---|------|
| <b>EAS2</b> | 30   | <100 | 1  | n.d. | 240 | 2000 | 9 | 5340 |
| <b>EAS3</b> | 1900 | 2200 | 23 | n.d. | 120 | 2490 | 3 | 120  |
|             |      |      |    |      |     |      |   |      |

XRF = X-Ray Fluorescence Spectrometry. n.d. = not detected

Elevated levels of titanium and iron correspond with rutile, hematite and magnetite. Higher levels of aluminium are due to plagioclase feldspar (e.g. albite).

## Appendix 2: Organic analyses of selected comminuted artificial stones (25 samples)

| Stone Type | Organic content<br>Calcination at 600C.<br>Percent loss | Organic content<br>Calcination at 600C.<br>After reaction with ALF for 8 weeks<br>Percent loss | Percentage of resin<br>lost after reaction with<br>ALF for 8 weeks | Loss on ignition<br>(1050C by XRF)<br>Percent loss |
|------------|---|--|--|--|
| AAS1       | 9.7   | n.a.   | n.a.   | 8.5  |
| AAS2       | 11.1  | 11.0   | 0.9  | 12.0   |
| AAS3       | 9.0   | n.a.   | n.a.   | n.a.   |
| AAS4       | 9.4   | 8.6  | 8.5  | 9.2  |
| AAS5       | 11.2  | n.a.   | n.a.   | n.a.   |
| AAS6       | 8.9   | 8  | 10.1   | 8.3  |
| AAS7       | 10.9  | 10.0   | 8.3  | 10.8   |
| AAS8       | 11.4  | n.a.   | n.a.   | n.a.   |
| BAS1       | 12.6  | n.a.   | n.a.   | 12.1   |
| BAS2       | 8.4   | n.a.   | n.a.   | 8.5  |
| BAS3       | 12.9  | n.a.   | n.a.   | 12.7   |
| BAS4       | 14.3  | 14.1   | 1.4  | 13.8   |

|             |      |      |      |      |
|-------------|------|------|------|------|
| <b>BAS5</b> | 12.6 | 11.7 | 7.1  | 12.1 |
| <b>BAS6</b> | 12.7 | n.a. | n.a. | n.a. |
| <b>BAS7</b> | 11.3 | n.a. | n.a. | n.a. |
| <b>BAS8</b> | 10.3 | 9.9  | 3.9  | 10.1 |
| <b>CAS1</b> | 11.9 | 10.9 | 8.4  | 11.8 |
| <b>CAS2</b> | 9.9  | 9.1  | 8.1  | 9.5  |
| <b>DAS1</b> | 9.7  | 9.6  | 1.0  | 10.4 |
| <b>DAS2</b> | 10.8 | 9.8  | 9.3  | 10.7 |
| <b>EAS1</b> | 14.6 | 13.5 | 7.5  | 14.5 |
| <b>EAS2</b> | 12.6 | 10.5 | 16.7 | 12.2 |
| <b>EAS3</b> | 12.7 | 11.9 | 6.3  | 12.3 |
| <b>FAS1</b> | 12.2 | n.a. | n.a. | 13.6 |
| <b>FAS2</b> | 14.3 | n.a. | n.a. | 11.8 |

XRF = X-Ray Fluorescence Spectrometry ; n.a. = not available

## Appendix 3: Time trends of metal ion release in Artificial Lysosomal Fluid (ALF)\*

Table A3.1: Data table for iron release (ug/L per gram of solid dust)

| Artificial Stone Type | Week 1 | Week 2 | Week 4 | Week 8 |
|-----------------------|--------|--------|--------|--------|
| AAS1                  | 4300   | 8116   | 10822  | 13296  |
| AAS2                  | 304    | 307    | 367    | 386    |
| BAS1                  | 67     | 86     | 95     | 88     |
| BAS2                  | 540    | 835    | 991    | 1257   |
| BAS3                  | 280    | 344    | 304    | 259    |
| BAS4                  | 98     | 106    | 107    | 116    |
| BAS5                  | 90     | 84     | 84     | 96     |
| CAS1                  | 87     | 76     | 72     | 75     |
| CAS2                  | 73     | 56     | 47     | 53     |
| DAS1                  | 1943   | 1807   | 1743   | 1526   |
| DAS2                  | 129    | 123    | 127    | 139    |
| EAS1                  | 82     | 94     | 86     | 88     |
| EAS2                  | 34     | 37     | 47     | 39     |
| EAS3                  | 3200   | 3677   | 4288   | 3909   |

Table A3.2: Data table for manganese release (ug/L per gram of solid dust)

| Artificial Stone Type | Week 1 | Week 2 | Week 4 | Week 8 |
|-----------------------|--------|--------|--------|--------|
| AAS1                  | 190    | 233    | 264    | 205    |
| AAS2                  | 24     | 20     | 19     | 14     |
| BAS2                  | 50     | 55     | 65     | 62     |
| BAS3                  | 29     | 29     | 29     | 22     |
| BAS4                  | 7      | 7      | 6      | 6      |
| BAS5                  | 8      | 5      | 4      | 3      |
| CAS1                  | 10     | 7      | 6      | 5      |
| CAS2                  | 5      | 5      | 4      | 4      |
| DAS1                  | 79     | 66     | 60     | 42     |
| DAS2                  | 17     | 14     | 13     | 10     |
| EAS1                  | 7      | 7      | 8      | 7      |
| EAS2                  | 2      | 2      | 4      | 3      |
| EAS3                  | 36     | 41     | 65     | 53     |

Table A3.3: Data table for aluminium release (ug/L per gram of solid dust)

| <b>Artificial Stone Type</b> | <b>Week 1</b> | <b>Week 2</b> | <b>Week 4</b> | <b>Week 8</b> |
|------------------------------|---------------|---------------|---------------|---------------|
| AAS1                         | 470           | 566           | 604           | 597           |
| AAS2                         | 1109          | 1307          | 1571          | 1293          |
| BAS1                         | 410           | 469           | 549           | 568           |
| BAS2                         | 620           | 714           | 767           | 796           |
| BAS3                         | 370           | 464           | 507           | 583           |
| BAS4                         | 364           | 409           | 410           | 350           |
| BAS5                         | 174           | 204           | 225           | 192           |
| CAS1                         | 486           | 592           | 654           | 527           |
| CAS2                         | 527           | 613           | 635           | 566           |
| DAS1                         | 284           | 367           | 389           | 288           |
| DAS2                         | 130           | 153           | 164           | 140           |
| EAS1                         | 128           | 131           | 191           | 134           |
| EAS2                         | 260           | 286           | 547           | 339           |
| EAS3                         | 134           | 135           | 243           | 174           |

Table A3.4: Data table for titanium release (ug/L per gram of solid dust)

| <b>Artificial Stone Type</b> | <b>Week 1</b> | <b>Week 2</b> | <b>Week 4</b> | <b>Week 8</b> |
|------------------------------|---------------|---------------|---------------|---------------|
| AAS1                         | 42            | 48            | 50            | 40            |
| AAS2                         | 93            | 82            | 88            | 76            |
| BAS1                         | 17            | 24            | 24            | 24            |
| BAS2                         | 13            | 18            | 18            | 19            |
| BAS3                         | 22            | 16            | 25            | 31            |
| BAS4                         | 13            | 14            | 14            | 14            |
| BAS5                         | 5             | 5             | 6             | 6             |
| CAS1                         | 11            | 11            | 11            | 10            |
| CAS2                         | 24            | 25            | 25            | 24            |
| DAS1                         | 34            | 33            | 31            | 24            |
| DAS2                         | 30            | 29            | 27            | 24            |
| EAS1                         | 2             | 2             | 3             | 2             |
| EAS2                         | 19            | 20            | 38            | 23            |
| EAS3                         | 7             | 8             | 15            | 10            |

\* In order to estimate the variability of quantified metal ion concentrations in ALF solutions, triplicate samples in separate bottles were run for two stone types (BAS2 and BAS4) across three time points (week 1, 2 and 4). The maximum coefficient of variation was 14.5% for Fe, 15.6% for Mn, 17% for Al and 22.8% for Ti.